Original Article

Evaluation of connective tissue disease-related interstitial lung disease using ultrasound elastography: a preliminary study

Songya Huang[1], Ruiqian Guo[1], Xinhui Yuan[2], Xinyi Tang[1], Tao Liu[3], Qibing Xie[3], Li Qiu[1]

[1]Department of Medical Ultrasound and National Clinical Research Center for Geriatrics, West China Hospital of Sichuan University, Chengdu, China; [2]Department of Medical Ultrasound, The People's Hospital of Leshan, Leshan, China; [3]Department of Rheumatology and Immunology, West China Hospital of Sichuan University, Chengdu, China

Contributions: (I) Conception and design: L Qiu, S Huang; (II) Administrative support: L Qiu; (III) Provision of study materials or patients: L Qiu, T Liu, Q Xie; (IV) Collection and assembly of data: S Huang, X Yuan, R Guo, X Tang; (V) Data analysis and interpretation: S Huang, L Qiu; (VI) Manuscript writing: All authors; (VII) Final approval of manuscript: All authors.

Correspondence to: Li Qiu. Department of Medical Ultrasound and National Clinical Research Center for Geriatrics, West China Hospital of Sichuan University, 37 Guo Xue Alley, Chengdu 610041, China. Email: qiulihx@scu.edu.cn.

Background: Interstitial lung disease (ILD) is a common pulmonary complication of connective tissue disease (CTD), which can lead to shortened survival. This article explores the ability of shear wave elastography (SWE) to assess lung surface elastic properties and to distinguish healthy lungs from diseased lungs with connective tissue disease-related interstitial lung disease (CTD-ILD). We aimed to determine whether SWE can be used to assess the severity of CTD-ILD.

Methods: A total of 65 CTD-ILD patients and 60 healthy volunteers were included for the case group and the control group, respectively. All participants underwent lung ultrasound (count of B-line and measurement of pleural line thickness) and SWE [measurement of Young's modulus (Emean) and shear wave velocity (SMV) (Cmean)] examinations at 50 lung sites. All participants also underwent an examination with high-resolution computed tomography (HRCT) and a pulmonary function test (PFT). For SWE assessment, the Q-box was set to its minimum size (1 mm) and manually placed on the pleural line, rather than inside the lung, to measure the stiffness of the lung surface. The intra- and inter-reliability of SWE measurements of healthy controls (HC), the receiver operating characteristic (ROC) curve for SWE for CTD-ILD, and correlations between different assessment methods were analyzed.

Results: Excellent intra- and inter-reliability of SWE measurements on the mid-anterior lung site of HCs (correlation coefficient >0.97; P<0.01) were found. The results of the lung ultrasound of case group participants were significantly higher than those of HCs at each site (P<0.001). The SWE results revealed a significant increase in both Emean and Cmean in CTD-ILD patients (P<0.001) compared with HCs at certain sites (P<0.001). The areas under the curve (AUC) of Emean and Cmean for CTD-ILD were 0.646 and 0.647 (P<0.05), respectively, and the cutoff values for Emean and Cmean to distinguish CTD-ILD from healthy lungs were 15.81 kPa and 2.31 m/s, respectively. There was no significant correlation between the SWE measured values and the number of B-lines, or the HRCT and PFT results, respectively (P>0.05).

Conclusions: As a noninvasive ultrasound elastography (UE) technique, SWE may provide a novel method to differentiate CTD-ILD-affected lungs and healthy lungs. It is a reliable way to measure the stiffness of a healthy lung surface in the supine position. However, the ability of SWE to evaluate the severity of CTD-ILD may be limited.

Keywords: Connective tissue disease-related interstitial lung disease (CTD-ILD); ultrasound elastography (UE); lung ultrasound; B-line; pleural line

Submitted Dec 16, 2021. Accepted for publication Apr 14, 2022.
doi: 10.21037/qims-21-1205
View this article at: https://dx.doi.org/10.21037/qims-21-1205

Introduction

Connective tissue disease (CTD) is a group of systemic autoimmune diseases characterized by immune-mediated tissue damage, which may affect many different organs and systems (1). Interstitial lung disease (ILD) is a pulmonary complication of CTD with a high morbidity and mortality. For example, the incidence of systemic sclerosis (SSc)-related ILD varies from 40% to 80%, depending on different ascertainments (2). In both SSc and rheumatoid arthritis (RA), the second leading cause of death is ILD (3). Therefore, it is essential to find more effective methods to diagnose and evaluate CTD-ILD.

Currently, the gold standard of medical imaging to diagnose ILD is high-resolution computed tomography (HRCT). However, due to the high amount of radiation, the application of HRCT is restricted in the early diagnosis and follow-up evaluation of CTD-ILD. In recent years, many studies have confirmed that lung ultrasound (LUS), as a noninvasive, convenient, and nonionizing radiation examination method, plays an important role in the evaluation of CTD-ILD (4-8). The count of B-lines and the evaluation of pleural line thickness and morphology have been employed as valuable parameters for CTD-ILD detection and follow-up (9,10). Nevertheless, B-lines are subjective assessments which can be influenced by operators' experience, and as nonspecific signs, they can be found in other interstitial changes of the lung (4,9). Furthermore, existing researches showed that ILD-induced lung fibrosis could result in stiffened lung tissue, which cannot be detected by either HRCT or LUS (11,12). To improve the detection and screening of ILD, it is important to seek quantitative and objective assessment methods for ILD and the potential stiffened lung tissue.

Ultrasound elastography (UE), a noninvasive technology, provides qualitative and quantitative tissue elasticity measurements to evaluate and diagnose disease. Strain elastography (SE), acoustic radiation force impulse (ARFI) technology, and shear wave elastography (SWE) are the main types of UE methods, and ARFI technology is divided into two parts: ARFI imaging, and quantitative ARFI methods (13). Both SE and ARFI imaging are semiquantitative methods to measure stiffness and obtain relative stiffness values. In contrast, the quantitative ARFI method and SWE use the acoustic radiation force emitted by the ultrasonic transducer to excite the tissue and generate shear waves. The shear wave velocity (SWV) is measured to quantitatively reflect the stiffness of the target tissue.

Various UE technologies have been applied to assess the stiffness of breast, thyroid, liver, muscle, and many other tissues or organs during evaluation and diagnosis (14-18). For lung diseases, there have only been a few studies in which UE was conducted to determine the stiffness of lung tumors and pleural effusion. Notably, a UE technology named lung ultrasound surface wave elastography (LUSWE) was proposed by Zhang *et al.* (19,20). This technology assesses lung surface elasticity by applying low-frequency harmonic vibrations, detecting lung surface waves with an ultrasound probe, and obtaining lung surface wave speed. It is mostly used to assess the lung elasticity of ILD patients. As mentioned above, lung tissue can eventually be damaged and stiffened with the progression of ILD-induced lung fibrosis (11,12). The peripheral and subpleural regions of the lung are major areas in which many ILDs typically distribute (12,21). These previous findings suggest that the elastic properties of lung surface tissue can be changed due to ILD. Therefore, using different UE tools to measure the surface elasticity of lungs affected by ILD could be possible and feasible.

To date, only Zhang *et al.* have researched LUSWE, and more work is needed to further clarify whether this technique is useful for patients with ILD. Among other UE technologies, SWE has the advantages of objective and quantitative measurements and a high level of repeatability. Moreover, there is still a lack of research on the application of SWE to evaluate the lungs of CTD-ILD patients and healthy people. Further research is also required to explore the reliability and repeatability of SWE measurements of lung surface stiffness and the value and significance of SWE assessment of CTD-ILD. We aimed to study the intra- and inter-reliability of SWE measurements on lung surface stiffness of healthy people, explore whether SWE can distinguish diseased patients from healthy controls (HCs), and determine whether SWE can be used to evaluate CTD-ILD by correlating it with other quantitative evaluation methods in this study. We present the following article in accordance with the GRRAS reporting checklist (available at https://qims.amegroups.com/article/view/10.21037/

Table 1 The 50-site examination protocol

Anatomical lines	50 sites		Position
	Right	Left	
Parasternal line	Second to fifth LIS	Second to fourth LIS	Supine
Midclavicular line	Second to fifth LIS	Second to fourth LIS	
Anterior axillary line	Second to fifth LIS	Second to fourth LIS	
Mid-axillary line	Second to fifth LIS	Second to fourth LIS	
Posterior axillary line	Seventh to eighth LIS	Seventh to eighth LIS	Sitting
Subscapular line	Seventh to eighth LIS	Seventh to eighth LIS	
Paravertebral line	Second to eighth LIS	Second to eighth LIS	

LIS, lung intercostal spaces.

qims-21-1205/rc).

Methods

Patients and controls

From March 2019 to November 2020, 65 patients diagnosed with CTD-ILD were consecutively recruited at the West China Hospital of Sichuan University according to the equation $n_1 = \frac{Z_\alpha^2 Sen(1-Sen)}{\delta^2}$, where n_1 is sample size, Z is statistic, α is confidence coefficient, Sen is sensitivity and δ is allowable error. A total of 60 healthy volunteers were enrolled at the West China Hospital of Sichuan University. This was approximate to the ratio of 1 patient to 1 volunteer. For the case group, patients with a history of respiratory diseases other than ILD, such as lung tumors and bulk pleural effusion, or with a history of other disorders (except for CTD) that may injure the respiratory system, such as heart disease, or with a history of medical treatment that may cause lung damage, such as radiotherapy and chemotherapy, were excluded from the study. For the control group, volunteers with a history of respiratory diseases, heart disease, rheumatic disease, or a history of medical treatment that may cause lung damage were excluded. Volunteers with respiratory symptoms and signs were excluded. Respiratory symptoms in volunteers were confirmed through a clinical examination performed by an experienced respiratory doctor. Meanwhile, pregnant women, people with skin scars at examination sites, and children (those under 18 years old) were not included in either group.

All recruited participants underwent LUS and SWE examinations. Additionally, all enrolled CTD-ILD patients were scheduled for an HRCT examination and received a pulmonary function test (PFT) within 30 days before or after the LUS and SWE examinations. Recruited CTD-ILD patients who could not complete the HRCT examination within the limited time were not included in the case group. The study was conducted in accordance with the Declaration of Helsinki (as revised in 2013). The study was approved by the Ethics Committee of the West China Hospital of Sichuan University, and informed consent was provided by all individual participants.

LUS and SWE examination

In this study, LUS and SWE examinations were performed using the Aixplorer US system (SuperSonic Imagine, Aix-en-Provence, France). An SL 10-2 linear probe (operating at 2–10 MHz), "General" mode, and the display scale (0–180 kPa) in the standard default setting were preselected. A total of 50 sites on two sides of the lung were all examined during LUS and SWE examination in the supine position and the seated position, as shown in *Table 1* and *Figure 1* (22). During the examination of each site, the probe tip was covered with ultrasound gel and gently and placed parallel to the lung intercostal spaces (LIS), perpendicular to the chest wall. No pressure was applied between the probe and chest wall skin. The B-lines were counted. A B-line was defined as a wedge-shaped hyperechoic artifact generated from the pleural line level extending to the edge of the screen (23) (*Figure 2*). The pleural line was defined as a horizontal hyperechoic line separating the chest wall and the lung, which can be observed to increase in ILD patients due to subpleural fibrotic scars (24). The measurement of the pleural line thickness was completed by sonographers when the B-mode image of the pleural line and the lung

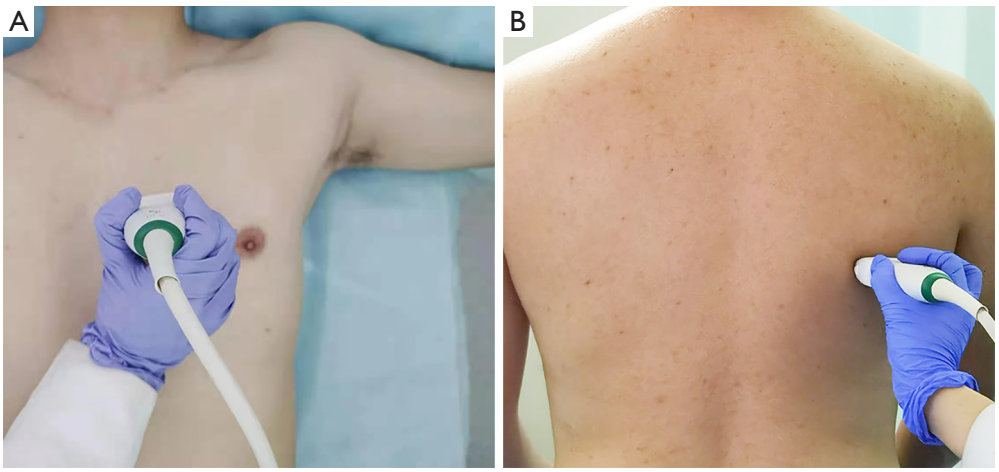

Figure 1 The position of the participant and the probe. (A) The third LIS of the left parasternal line examined in the supine position (with both upper limbs abducted at 90 degrees); (B) the seventh LIS of the right subscapular line in the sitting position (with both upper limbs naturally placed on both sides of the body); the probe was placed perpendicularly to the chest wall, parallel to the lung intercostal space. LIS, lung intercostal space.

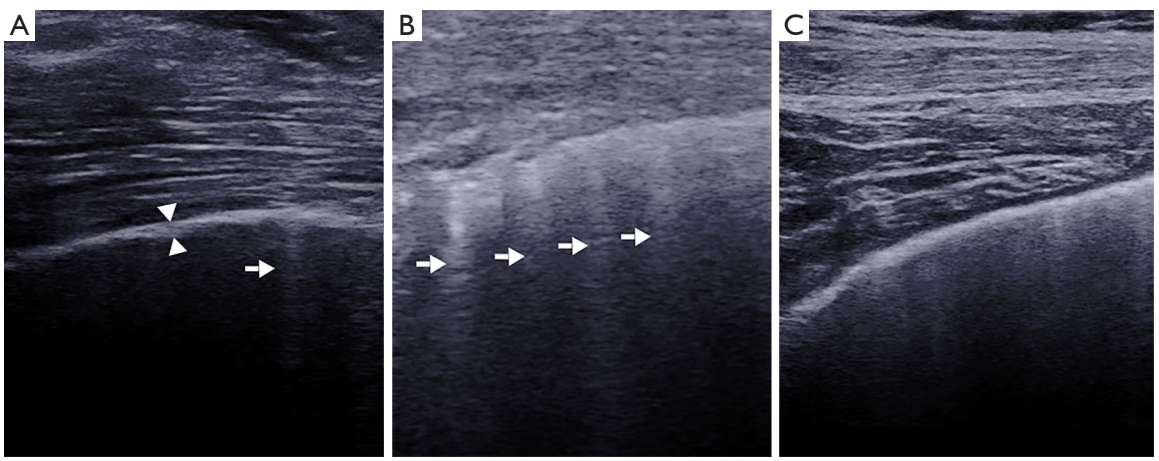

Figure 2 B-mode images of B-lines and the pleural line. (A) 1 B-line indicated by a white arrow and the pleural line (shown as a continuous line with high echo) indicated by white triangles. (B) 4 B-lines indicated by white arrows. (C) Full white screen.

below were clearly shown on the screen (*Figure 2*). If there was a full white screen or a total of more than 10 B-lines in a single scanning site, the count of B-lines was recognized as 10 B-lines (25). Maximal contrast between all evaluated structures was obtained by manually adjusting image parameters (26).

After switching to SWE mode, efforts were made to ensure that the central area of the real-time color-coded square region of interest (ROI) overlay on the grayscale image was placed at the pleural line level. In the meantime, the transducer remained stable. The participants were asked to take a deep breath and hold their breath for a few seconds at the end of the maximum inspiration to obtain a stable SWE image. The Q-box, a small circle, was placed on the pleural line (close to the middle line of the screen) to measure the lung surface stiffness. As ILD-induced abnormalities are frequently distributed in subpleural areas (11), the pleural line was defined as a horizontal hyperechoic line that separates the chest wall from the lung with increased thickness, and the irregularity is related to subpleural fibrotic scars (24). Therefore, pleural line stiffness was considered to correspond to lung surface

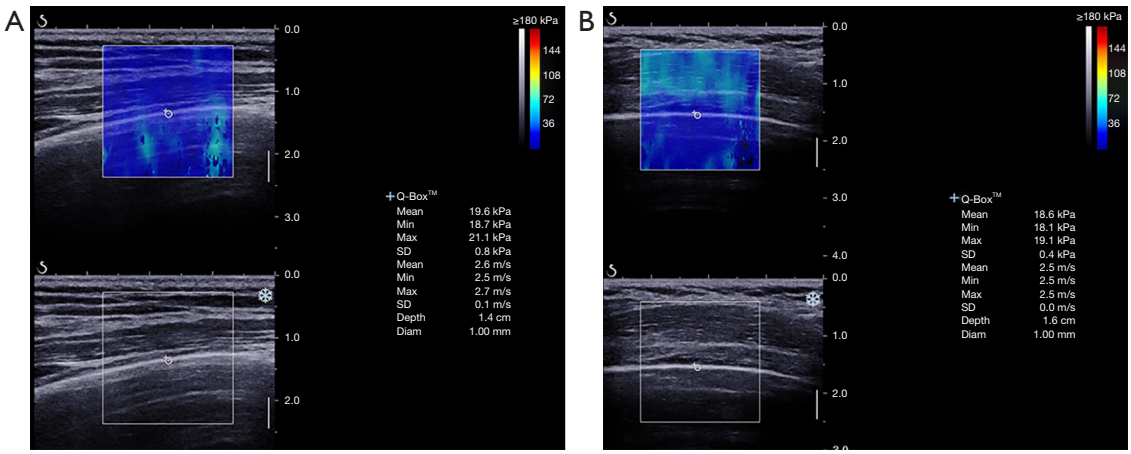

Figure 3 SWE image of pleural line. (A) SWE measurement of the fourth LIS of the left posterior axillary line; (B) SWE measurement of the third LIS of the right parasternal line. SWE, shear wave elastography; LIS, lung intercostal space.

Table 2 Warrick scoring method (27)

HRCT abnormalities	Severity	Extent of disease—lung segments involved		
		1–3	4–9	>9
Ground glass opacities	1	1	2	3
Irregular pleural margin	2	1	2	3
Septal or subpleural lines	3	1	2	3
Subpleural cyst	4	1	2	3
Honeycomb	5	1	2	3

HRCT, high-resolution computed tomography.

stiffness. The diameter of the Q-box was set to its minimum size (1 mm), and, if the thickness of the pleural line was less than 1 mm, the Q-box should include the pleural line and part of the lung surface below. The image displayed the mean, maximum, minimum, and standard deviation values of the elastic moduli, including both Young's modulus and SWV. These were automatically calculated and presented by the system according to the equation $E = 3\rho c^2$ (E = Young's modulus, ρ = tissue density, c = SWV) (*Figure 3*). In this study, three measurements were taken at each site. The mean Young's modulus value and the mean SWV value were representative values that we selected in each obtained measurement. Then, the averaged mean value of Young's modulus (Emean, kPa) and the averaged mean value of SWV (Cmean, m/s) of the pleural line were recorded.

The SWE examination was performed and interpreted by sonographer A and sonographer B, each with at least 3 years' experience examining musculoskeletal system and lungs, who were blinded to each other's interpretation throughout the whole study. All participants were examined by sonographer A independently, while the third LIS of the right midclavicular line of 20 randomly selected healthy participants was examined again by sonographer B independently on the same day to assess inter-operator variability. For the assessment of intra-operator variability, repeated SWE measurements of the third LIS of the right midclavicular line of these 20 participants were performed independently by sonographer A one week later.

HRCT assessment

The HRCT examinations were conducted with computed tomography (CT) scanners from Siemens (Siemens Healthineers, Erlangen, Germany), Philips (Philips, Best, The Netherlands), and GE (GE Healthcare, Milwaukee, WI, USA) according to the standard protocol. The whole lung (from the apex to the base) was scanned at full inspiration with the participants in the supine position. The slice thickness and spacing of scans were both 1 mm. The HRCT images were interpreted and scored by an experienced radiologist who was blinded to the PFTs, LUS, and SWE findings according to the Warrick scoring method (score range: 0 to 30) (27) (*Table 2*).

The PFT

A PFT was performed using the Masterscreen pulmonary

Table 3 Demographic and clinical characteristics of all recruited participants

Characteristics	Case group (n=65)	Control group (n=60)	P value
CTD classification		/	/
SSc	23		
IIM	22		
ASS	6		
MCTD	3		
SS	3		
RA	2		
RA + SSc	2		
UCTD	2		
AAV	1		
SLE	1		
Age, years, mean ± SD	49.14±10.97	46.53±12.61	0.219
Gender, male/female	20/45	19/41	0.914
BMI, kg/m^2, mean ± SD	22.91±3.55	22.54±2.78	0.517
Smoke (yes/no)	10/55	7/53	0.545

CTD, connective tissue disease; SSc, systemic sclerosis; IIM, idiopathic inflammatory myopathy; ASS, anti-synthetase syndrome; MCTD, mixed CTD; SS, Sjogren's syndrome; RA, rheumatic arthritis; UCTD, undifferentiated CTD; AAV, anti-neutrophil cytoplasmic antibody-associated vasculitis; SLE, systemic lupus erythematosus; BMI, body mass index.

function measurement system (Jaeger, Wuerzburg, Germany). Forced vital capacity (FVC) and diffusing capacity of the lung for carbon monoxide (DLCO) were chosen as indicators for further analysis in this study, and were expressed as percentages of predicted values.

Statistical analysis

Statistical analysis was carried out using SPSS 20.0 software (IBM Corp., Armonk, NY, USA). In this study, continuous variables were presented as the mean ± standard deviation for data with normal distributions and as the median (upper quartile, lower quartile) for data with abnormal distributions. Categorical variables were expressed as numbers and percentages. The demographic data statistics of the control group and the CTD-ILD group were determined using the χ^2 test and *t*-test for continuous variables and categorical variables, respectively. Additionally, the receiver operating characteristic (ROC) curve, area under the curve (AUC), and cutoff values with associated sensitivity and specificity were analyzed. The comparison of the pleural line elasticity between the control group and the CTD-ILD group was undertaken using the Mann–Whitney U rank sum test. Pearson's correlation analysis (r) was used to determine the relation between the pleural line elasticity, including both Emean and Cmean, and to interpret the results of LUS, HRCT, and PFTs. The single-measure intraclass correlation coefficient (ICC) using a two-way random-effects model and absolute type was used in intra- and interobserver repeatability assessments. Consistency analysis was conducted using Pearson's correlation. A two-sided P value of <0.05 was considered statistically significant.

Results

We enrolled 65 CTD-ILD patients and 60 HCs according to the criteria mentioned previously. All HCs were confirmed to have no respiratory symptoms or signs by clinical examination. In the case group, most patients were diagnosed with either SSc (n=23) or idiopathic inflammatory myopathy (IIM) (n=22). There was no statistically significant difference between the CTD-ILD case group and the control group in terms of gender, age, body mass index (BMI), or smoking status. The detailed demographic and clinical characteristics of all participants are shown in *Table 3*.

Reliability of SWE measurements

Table 4 illustrates the intra- and inter-observer repeatability of the SWE quantification in the third LIS pleural line of the right midclavicular line of 20 HCs. The interobserver reliability was evaluated with two sonographers' measurements in this study. For both Emean and Cmean, the ICC value was >0.97 for intra- and inter-observer reliability (P<0.01). The R^2 value was also >0.96 (P<0.01), which showed the correlation of intra- and inter-observer ICCs analogously (*Figure 4*).

Comparison of LUS and SWE measurements between the case group and the control group

The LUS and SWE examinations were scheduled for a total of 3,250 sites in 65 cases, of which 100 sites could not be scanned or measured because they were covered

Table 4 Intra- and inter-observer reliability of quantitative lung stiffness SWV measurements

SWE measurements	Sonographer A1	Sonographer A2	Sonographer B	ICC (95% confidence interval)		P value
				Intraobserver	Interobserver	
Cmean (m/s)†	2.26±0.34	2.27±0.32	2.27±0.30	0.986 (0.966–0.994)	0.976 (0.941–0.969)	<0.01*
Emean (kPa)†	15.74±4.79	15.67±4.64	15.73±4.47	0.998 (0.994–0.999)	0.994 (0.985–0.998)	<0.01*

†, mean ± standard deviation; *, P<0.01. SWV, shear wave velocity; SWE, shear wave elastography; Emean, averaged mean Young's modulus; Cmean, averaged mean shear wave velocity; Sonographer A1, first measurement of Sonographer A; Sonographer A2, second measurement of sonographer A; ICC, intraclass correlation coefficient.

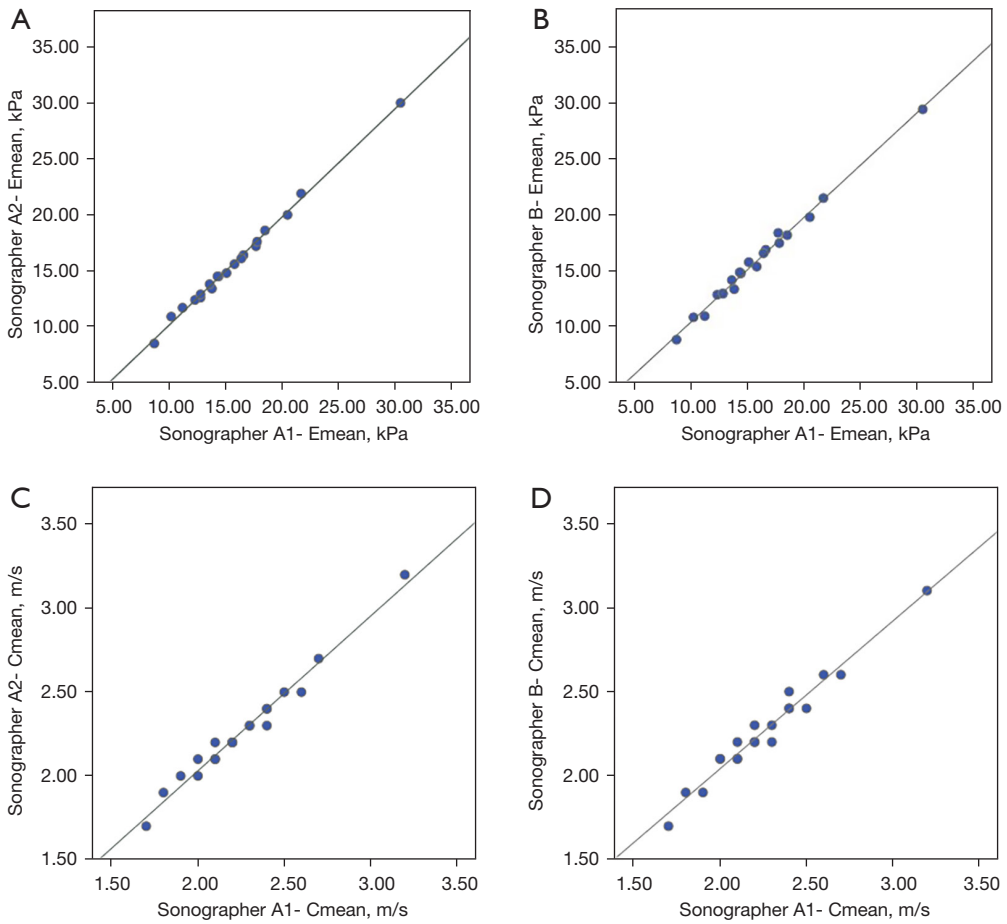

Figure 4 Intra- and inter-observer reliability of quantitative lung surface stiffness shear wave elastography measurements (P<0.01). (A) Intraobserver reliability in Young's modulus. (B) Interobserver reliability in Young's modulus. (C) Intraobserver reliability in SWV. (D) Interobserver reliability in SWV. Emean, averaged mean Young's modulus; Cmean, averaged mean SWV. SWV, shear wave velocity.

by different organs, such as the liver, spleen, or heart. Moreover, there were 2 sites that were not measured by SWE due to the deep location of the pleural line. In addition, there were 4 sites where the pleural line thickness could not be measured due to the extreme irregularity of the pleural line. For the control group, a total of 3,000 sites in 60 healthy volunteers were examined by LUS and SWE. The number of B-lines, pleural line thickness, and Emean and Cmean of the pleural line in the case group were generally higher than those of the HCs, and the difference

Table 5 Comparison of shear wave elastography measurements between the case group and the control group

Parameters	The case group (n=3,148)	The control group (n=3,000)	P value
Emean (kPa)	17.90 (12.20, 25.68)	15.20 (12.30, 18.40)	<0.001*
Cmean (m/s)	2.40 (2.00, 2.90)	2.20 (2.00, 2.50)	<0.001*

Data are presented as the median (upper quartile, lower quartile). *, P<0.001. Emean, averaged mean Young's modulus; Cmean, averaged mean shear wave velocity.

Table 6 Comparison of LUS measurements (number of B-lines) between the case group and the control group

Parameters	The case group (n=3,150)	The control group (n=3,000)	P value
Number of B-lines	0.00 (0.00, 2.00)	0.00 (0.00, 0.00)	<0.001*

Data are presented as the median (upper quartile, lower quartile). *, P<0.001. LUS, lung ultrasound; H, pleural line thickness.

Table 7 Comparison of LUS measurements (pleural line thickness) between the case group and the control group

Parameters	The case group (n=3,146)	The control group (n=3,000)	P value
H (mm)	1.10 (0.80, 1.40)	0.70 (0.70, 0.80)	<0.001*

Data are presented as the median (upper quartile, lower quartile). *, P<0.001. LUS, lung ultrasound; H, pleural line thickness.

was statistically significant (P<0.001) (*Tables 5*-7; *Figure 5*). Comparison of each parameter between the case group and the HC group at each site showed that more B-lines and thicker pleural lines were found in the CTD-ILD group at all 50 sites (Table S1; Table S2), while statistically higher Emean and Cmean of the case group were only found in the following 22 sites (P<0.05): the fifth LIS of the right parasternal line and right anterior axillary line, the second to fifth LIS of the right midclavicular line, the fourth LIS of the bilateral midaxillary line, the eighth LIS of the right posterior axillary line, the second to fourth LIS of the right paravertebral line, the second to fourth LIS of the left midclavicular line, the third and fourth LIS of the left anterior axillary line and the second to sixth LIS of the left paravertebral line (Table S3; Table S4). Additionally, at the second LIS of the bilateral midclavicular line and of the left midaxillary line, the Cmean of CTD-ILD cases was higher than that of HCs (P<0.05), and statistically higher values of the pleural line Young's modulus of CTD-ILD cases were found at the fifth LIS of the right paravertebral line (P<0.05).

Analysis of ROC curve for SWE measurements for CTD-ILD

The AUC of Emean and Cmean for assessing CTD-ILD were 0.646 and 0.647, respectively. This indicated that the diagnostic value of SWE measurements for CTD-ILD was acceptable (*Figure 6*). The cutoff values for Emean and Cmean were 15.81 kPa and 2.31 m/s, respectively, which could help distinguish CTD-ILD from healthy lungs (*Table 8*).

Quantitative SWE measurements of the case group in relation to the LUS interpretation

In the case group, two SWE values related to pleural line elasticity and the number of B-lines had no significant correlations (P>0.05), while a weakly negative correlation was found between Emean and Cmean of the pleural line and the pleural line thickness (r=−0.284 and r=−0.316, respectively, P<0.05). The results are outlined in *Table 9*. For meaningful sites (a total of 22 sites) which had a difference in both pleural line elastic moduli between cases and HCs, the values of the pleural line Young's modulus and SWV were extracted and analyzed. Those values still had no relation to the number of B-lines (P>0.05). Similarly, Emean (r=−0.245; P<0.05) and Cmean (r=−0.269; P<0.05) of the pleural line were negatively associated with pleural line thickness (*Table 10*).

Quantitative SWE measurements of the case group in relation to the HRCT and PFT results

The average Warrick score of all 65 CTD-ILD patients was 14.43±6.60. Regarding PFTs, 25 patients did not undergo

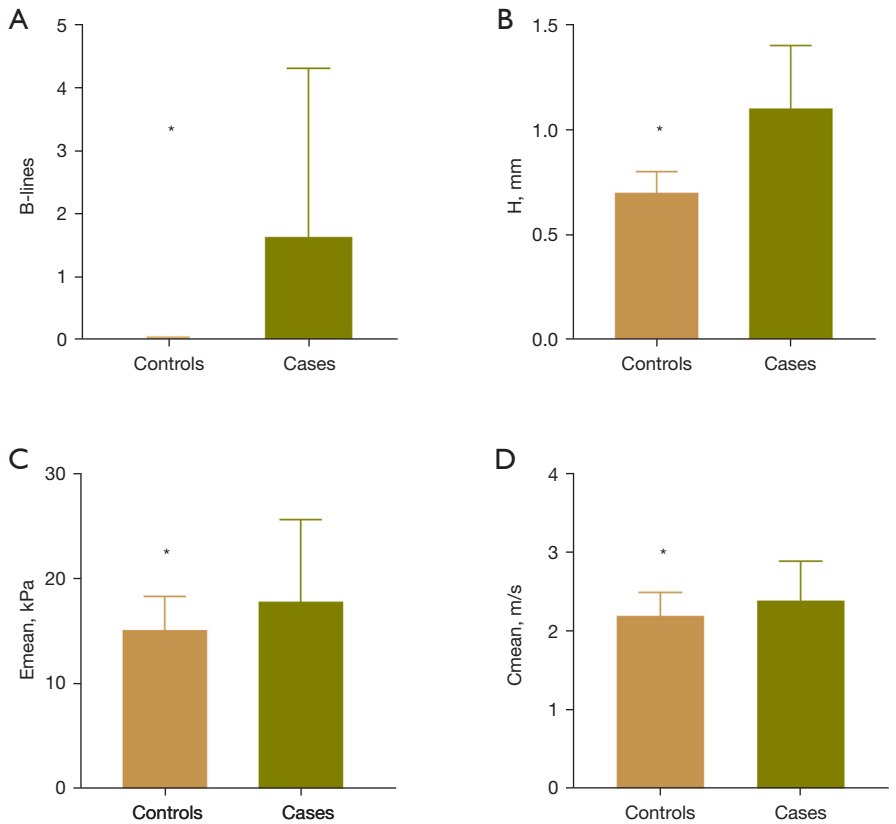

Figure 5 Comparison SWE and LUS measured values between the case group and the control group. (A) Comparison of the number of B-lines. (B) Comparison of the pleural line thickness. (C) Comparison of the pleural line Young's modulus. (D) Comparison of the pleural line SWV. *, P<0.05. Cmean, averaged mean shear wave velocity; Emean, averaged mean Young's modulus; SWE, shear wave elastography; SWV, shear wave velocity; LUS, lung ultrasound.

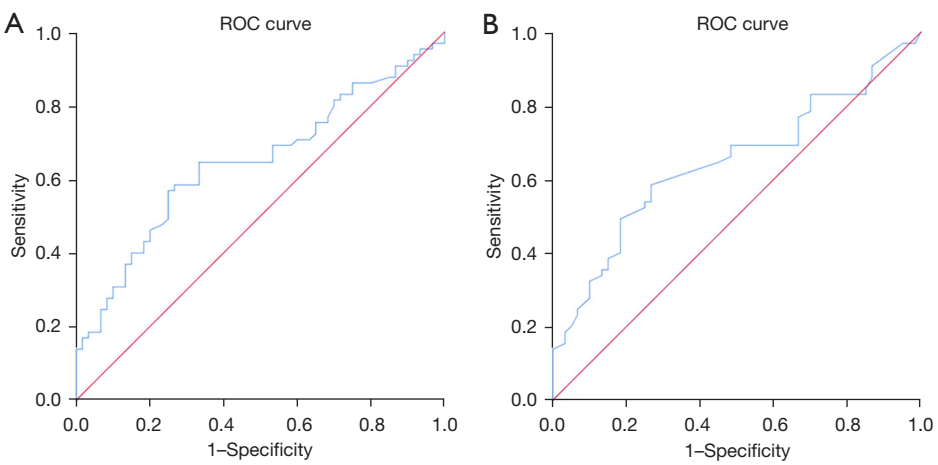

Figure 6 ROC curves for SWE measurements. (A) ROC curves for pleural line Young's modulus for CTD-ILD. (B) ROC curves for pleural line SWV for CTD-ILD. ROC, receiver operating characteristic; SWE, shear wave elastography; CTD-ILD, connective tissue disease-related interstitial lung disease.

Table 8 Diagnostic accuracy of SWE measurements for CTD-ILD

Parameters	AUC (95% CI)	Standard error[a]	P[b]	Cutoff value	Sensitivity	Specificity	95% CI
Emean (kPa)	0.646 (0.549–0.743)	0.050	0.005*	15.81	0.646	0.667	0.549–0.743
Cmean (m/s)	0.647 (0.549–0.744)	0.050	0.005*	2.31	0.585	0.733	0.549–0.744

[a], under the nonparametric assumption; [b], null hypothesis: true area =0.5. *, P<0.05. SWE, shear wave elastography; CTD-ILD, connective tissue disease-related interstitial lung disease; Emean, averaged mean Young's modulus; Cmean, averaged mean shear wave velocity; AUC, area under the curve; CI, confidence interval.

Table 9 Relationship between shear wave elastography measurements and lung ultrasound evaluation results at 50 sites

Parameters	The number of B-line		H (mm)	
	r	P value	r	P value
Emean (kPa)	0.053	>0.05	−0.284*	<0.05
Cmean (m/s)	0.044	>0.05	−0.316*	<0.05

*, P<0.05. H, pleural line thickness; Emean, averaged mean Young's modulus; Cmean, averaged mean shear wave velocity.

Table 10 Relationship between shear wave elastography measurements and lung ultrasound evaluation results at 22 sites

Parameters	The number of B-line		H (mm)	
	r	P value	r	P value
Emean (kPa)	0.025	>0.05	−0.245*	<0.05
Cmean (m/s)	0.033	>0.05	−0.269*	<0.05

*, P<0.05. H, pleural line thickness; Emean, averaged mean Young's modulus; Cmean, averaged mean shear wave velocity.

Table 11 Relationship between shear wave elastography measurements and HRCT and PFT results at 50 sites

Parameters	HRCT (n=65), r (P)	PFT (n=37), r (P)	
	Warrick score	FVC, %	DLCO, %
Emean (kPa)	−0.010 (>0.05)	0.040 (>0.05)	0.305 (>0.05)
Cmean (m/s)	−0.015 (>0.05)	0.025 (>0.05)	0.306 (>0.05)

HRCT, high-resolution computed tomography; PFT, pulmonary function test; FVC, forced vital capacity; DLCO, diffusing capacity of the lung for carbon monoxide; H, pleural line thickness; Emean, averaged mean Young's modulus; Cmean, averaged mean shear wave velocity.

Table 12 Relationship between shear wave elastography measurements and HRCT and PFT results at 22 sites

Parameters	HRCT (n=65), r (P)	PFT (n=37), r (P)	
	Warrick score	FVC, %	DLCO, %
Emean (kPa)	−0.053 (>0.05)	−0.018 (>0.05)	0.279 (>0.05)
Cmean (m/s)	−0.040 (>0.05)	−0.005 (>0.05)	0.319 (>0.05)

HRCT, high-resolution computed tomography; PFT, pulmonary function test; FVC, forced vital capacity; DLCO, diffusing capacity of the lung for carbon monoxide; H, pleural line thickness; Emean, averaged mean Young's modulus; Cmean, averaged mean shear wave velocity.

the examination in time, and 3 patients could not complete the whole examination process to obtain full results. Therefore, only 37 patients successfully underwent PFTs. The average values of FVC and DLCO were 87.5%±17.2% and 72.6%±17.7%, respectively. *Table 11* shows that there was no significant correlation between Emean and Cmean of the pleural line and Warrick score in the case group (r=−0.010 and r=−0.015, respectively, P>0.05). Similarly, no significant correlation was found between the pleural line elastic values and PFT results (P>0.05; *Table 11*). Moreover, in the 22 meaningful sites, the pleural line elastic values had no significant relation to the HRCT assessment of the PFT results (P>0.05; *Table 12*).

Discussion

As reported, changes in biomechanical properties of the lung can be found in some lung diseases, such as ILD (12). Many types of ILDs distributed in the subpleural regions can lead to stiffened lung surface tissue (12). Observation of the change in lung surface stiffness may help diagnose ILD. Currently, HRCT is the gold standard of medical imaging for ILD diagnosis, and LUS plays an important role in the evaluation of CTD-ILD. However, the high radiation dose restrains the application of HRCT. Furthermore, the B-line is a nonspecific sign of interstitial lung processes, which decreases the diagnostic specificity for CTD-ILD of LUS. Moreover, both methods are not capable of examining the

stiffened lung surface tissue that occurs with lung fibrosis. As a noninvasive technology that can quantitatively measure tissue stiffness, SWE may provide a promising and novel method to assess CTD-ILD.

Although SWE has been used to quantify the stiffness of the skin, liver, and breast masses, and the consistency analysis results have been optimistic (28-30), no previous studies have investigated the reliability and repeatability of SWE measurements on lung surface stiffness. In the present study, intra- and inter-group consistency for examining the lung surface stiffness of the mid-anterior lung site of 20 volunteers was performed and the results were excellent. However, only one site in a HC was chosen to perform the repeated SWE examination. This site was the most superficial and the technically simplest site to obtain and was examined only in the supine position, which cannot indicate how the depth of different lung sites and the body habitus may influence the consistency results. Moreover, CTD-ILD patients were not included in the consistency analysis. Different results may be obtained from CTD-ILD patients because of their more complicated situations, such as tachypnea or difficulties obtaining lung imaging, which may influence the results. Therefore, the results in the present study only indicated that the repeatability of SWE measurements on healthy lung surface stiffness in the supine position was excellent (*Table 4*; *Figure 4*). These limitations need to be further studied. We also found that not all selected sites of each patient could be detected during the examination because they were covered by adjacent organs, which is similar to the situation mentioned by Vassalou *et al.* (26). The number of B-lines and the pleural line thickness between the case group and the HC group were significantly different both in the overall 50-site scheme and at each site, and the measured values in the case group were greater, which is consistent with many other studies (31,32). In addition, the values of the pleural line Young's modulus and SWV of the case group were higher than those of the control group at certain sites (*Tables 8*,*9*). Other studies that have used LUSWE to evaluate lung surface stiffness in patients with ILD (mostly SSc-ILD) and in healthy people have indicated that the lung surface wave velocity in ILD patients is higher than that in HCs (11,12,33,34). The results of those studies are similar to those of the present study, which all implied that the ILD-affected lung is stiffer than the normal lung. Therefore, the pleural line Young's modulus and SWV may provide new indicators to distinguish healthy lungs from lungs with ILD. Sites where stiffness quantification values were significantly different between cases and controls may be potential examination sites to differentiate between healthy and diseased lungs when using SWE, while the pathophysiologic and other influencing factors should be considered. Nevertheless, to the best of our knowledge, there have been no other studies on SWE measurements of the lungs affected by CTD-ILD. However, in view of the limited number of recruited participants, more research is still needed for further exploration. The ROC curve suggested that SWE values can be used to distinguish CTD-ILD and healthy lungs with passable diagnostic efficacy. Furthermore, the calculated cutoff values of both Emean and Cmean may be used as cutoff values for distinguishing CTD-ILD from healthy lungs. Nevertheless, we also found that the sensitivity and specificity associated with these cutoff values were not very high. In view of the relatively low number of enrolled cases and HCs, the analysis of the ROC curve can be reference only, and further study is needed.

In the present study, the values measured using SWE, namely, Young's modulus and SWV of the pleural line, showed weakly negative correlations with pleural line thickness (*Tables 9*,*10*). This weak correlation suggests that these may be considered to have no specific clinical significance. Furthermore, when examining the relationship between SWE measurements and other methods that are useful in the diagnosis and evaluation of CTD-ILD, the study found that SWE elastic moduli had no relation to other parameters to evaluate LUS (the number of B-lines) or interpreting the results of HRCT and PFTs in both the 50-site protocol and 22 selected sites. According to the above results, we consider that SWE assessment of the severity of CTD-ILD may be of limited value. We suppose that the SWE measurement of lung surface stiffness may be influenced by many factors, such as age, BMI, adjacent organs, and different examination areas, which may result in nonsignificant correlations between SWE results and other evaluation methods. These relationships need to be further studied. In consideration of the uncertain influencing factors and the lack of similar studies, the value of SWE for CTD-ILD evaluation needs to be further explored and confirmed.

There are some other limitations to the current study. First, an analysis of factors that influenced SWE measurements of lung surface stiffness was not included in the study. When the pleural line thickness of the participant was less than 1 mm, the Q-box (minimum diameter of 1 mm) in the SWE examination contained the pleural line and the lung surface below it. This measuring method

may affect the SWE quantification of the pleural line and needs to be further studied and improved. Moreover, 30 days between LUS/SWE and HRCT examinations may cause dramatically different results between different examinations after induction steroid therapy and other treatments. Although the mean interval between LUS/SWE and HRCT was 4.17 days in the present study, which may not cause obvious dyssynchrony of the LUS/SWE and HRCT results, the interval may need to be reduced in future research. Finally, because this study is a preliminary study, CTD-ILD patients were not grouped in accordance to different CTD types to compare the LUS and SWE data. In the future, these limitations need to be further addressed.

Conclusions

In addition to LUS, which can be used to evaluate CTD-ILD and distinguish CTD-ILD-affected lungs from healthy lungs, SWE can also be performed to measure the lung surface stiffness of CTD-ILD patients and HCs to differentiate them at certain sites. Cutoff values were calculated to help the differentiation. Moreover, measurement of healthy anterior lung surface stiffness in the supine position was found to be a reliable approach. This result suggested that SWE may provide a promising imaging method to assess lung surface stiffness. However, the value of SWE assessment for the severity of CTD-ILD is limited in the present study, and further study of the ability and reliability of SWE for lung surface stiffness assessment is needed.

Acknowledgments

Funding: This work was supported by the 1·3·5 Project for Disciplines of Excellence–Clinical Research Incubation Project (No. 2020HXFH001) and the National Clinical Research Center for Geriatrics (No. Z2021LC002).

Footnote

Reporting Checklist: The authors have completed the GRRAS reporting checklist. Available at https://qims.amegroups.com/article/view/10.21037/qims-21-1205/rc

Conflicts of Interest: All authors have completed the ICMJE uniform disclosure form (available at https://qims.amegroups.com/article/view/10.21037/qims-21-1205/coif). The authors have no conflicts of interest to declare.

Ethical Statement: The authors are accountable for all aspects of the work in ensuring that questions related to the accuracy or integrity of any part of the work are appropriately investigated and resolved. The study was conducted in accordance with the Declaration of Helsinki (as revised in 2013). The study was approved by the Ethics Committee of the West China Hospital of Sichuan University, and informed consent was provided by all individual participants.

References

1. Mira-Avendano I, Abril A, Burger CD, Dellaripa PF, Fischer A, Gotway MB, Lee AS, Lee JS, Matteson EL, Yi ES, Ryu JH. Interstitial Lung Disease and Other Pulmonary Manifestations in Connective Tissue Diseases. Mayo Clin Proc 2019;94:309-25.
2. Gutsche M, Rosen GD, Swigris JJ. Connective Tissue Disease-associated Interstitial Lung Disease: A review. Curr Respir Care Rep 2012;1:224-32.
3. Salaffi F, Carotti M, Baldelli S, Bichi Secchi E, Manganelli P, Subiaco S, Salvolini L. Subclinical interstitial lung involvement in rheumatic diseases. Correlation of high resolution computerized tomography and functional and cytologic findings. Radiol Med 1999;97:33-41.
4. Wang Y, Gargani L, Barskova T, Furst DE, Cerinic MM. Usefulness of lung ultrasound B-lines in connective tissue disease-associated interstitial lung disease: a literature review. Arthritis Res Ther 2017;19:206.
5. Ferro F, Delle Sedie A. The use of ultrasound for assessing interstitial lung involvement in connective tissue diseases. Clin Exp Rheumatol 2018;36 Suppl 114:165-70.
6. Xie HQ, Zhang WW, Sun S, Chen XM, Yuan SF, Gong ZH, Liu L. A simplified lung ultrasound for the diagnosis of interstitial lung disease in connective tissue disease: a meta-analysis. Arthritis Res Ther 2019;21:93.
7. Volpicelli G. Lung Ultrasound B-Lines in Interstitial Lung Disease: Moving From Diagnosis to Prognostic

Stratification. Chest 2020;158:1323-4.
8. Vicente-Rabaneda EF, Bong DA, Castañeda S, Möller I. Use of ultrasound to diagnose and monitor interstitial lung disease in rheumatic diseases. Clin Rheumatol 2021;40:3547-64.
9. Fairchild R, Chung M, Yang D, Sharpless L, Li S, Chung L. Development and Assessment of Novel Lung Ultrasound Interpretation Criteria for the Detection of Interstitial Lung Disease in Systemic Sclerosis. Arthritis Care Res (Hoboken) 2021;73:1338-42.
10. Pinal-Fernandez I, Pallisa-Nuñez E, Selva-O'Callaghan A, Castella-Fierro E, Simeon-Aznar CP, Fonollosa-Pla V, Vilardell-Tarres M. Pleural irregularity, a new ultrasound sign for the study of interstitial lung disease in systemic sclerosis and antisynthetase syndrome. Clin Exp Rheumatol 2015;33:S136-41.
11. Clay R, Bartholmai BJ, Zhou B, Karwoski R, Peikert T, Osborn T, Rajagopalan S, Kalra S, Zhang X. Assessment of Interstitial Lung Disease Using Lung Ultrasound Surface Wave Elastography: A Novel Technique With Clinicoradiologic Correlates. J Thorac Imaging 2019;34:313-9.
12. Zhang X, Osborn T, Zhou B, Meixner D, Kinnick RR, Bartholmai B, Greenleaf JF, Kalra S. Lung Ultrasound Surface Wave Elastography: A Pilot Clinical Study. IEEE Trans Ultrason Ferroelectr Freq Control 2017;64:1298-304.
13. Shiina T, Nightingale KR, Palmeri ML, Hall TJ, Bamber JC, Barr RG, et al. WFUMB guidelines and recommendations for clinical use of ultrasound elastography: Part 1: basic principles and terminology. Ultrasound Med Biol 2015;41:1126-47.
14. Yin L, Cheng L, Wang F, Zhu X, Hua Y, He W. Application of intraoperative B-mode ultrasound and shear wave elastography for glioma grading. Quant Imaging Med Surg 2021;11:2733-43.
15. Jia W, Luo T, Dong Y, Zhang X, Zhan W, Zhou J. Breast Elasticity Imaging Techniques: Comparison of Strain Elastography and Shear-Wave Elastography in the Same Population. Ultrasound Med Biol 2021;47:104-13.
16. Tang X, Wang L, Guo R, Huang S, Tang Y, Qiu L. Application of ultrasound elastography in the evaluation of muscle strength in a healthy population. Quant Imaging Med Surg 2020;10:1961-72.
17. Qiu Y, Xing Z, Liu J, Peng Y, Zhu J, Su A. Diagnostic reliability of elastography in thyroid nodules reported as indeterminate at prior fine-needle aspiration cytology (FNAC): a systematic review and Bayesian meta-analysis. Eur Radiol 2020;30:6624-34.
18. Nierhoff J, Chávez Ortiz AA, Herrmann E, Zeuzem S, Friedrich-Rust M. The efficiency of acoustic radiation force impulse imaging for the staging of liver fibrosis: a meta-analysis. Eur Radiol 2013;23:3040-53.
19. Zhang X, Osborn T, Kalra S. A noninvasive ultrasound elastography technique for measuring surface waves on the lung. Ultrasonics 2016;71:183-8.
20. Zhang X, Qiang B, Hubmayr RD, Urban MW, Kinnick R, Greenleaf JF. Noninvasive ultrasound image guided surface wave method for measuring the wave speed and estimating the elasticity of lungs: A feasibility study. Ultrasonics 2011;51:289-95.
21. Desai SR, Veeraraghavan S, Hansell DM, Nikolakopolou A, Goh NS, Nicholson AG, Colby TV, Denton CP, Black CM, du Bois RM, Wells AU. CT features of lung disease in patients with systemic sclerosis: comparison with idiopathic pulmonary fibrosis and nonspecific interstitial pneumonia. Radiology 2004;232:560-7.
22. Tardella M, Gutierrez M, Salaffi F, Carotti M, Ariani A, Bertolazzi C, Filippucci E, Grassi W. Ultrasound in the assessment of pulmonary fibrosis in connective tissue disorders: correlation with high-resolution computed tomography. J Rheumatol 2012;39:1641-7.
23. Gutierrez M, Salaffi F, Carotti M, Tardella M, Pineda C, Bertolazzi C, Bichisecchi E, Filippucci E, Grassi W. Utility of a simplified ultrasound assessment to assess interstitial pulmonary fibrosis in connective tissue disorders--preliminary results. Arthritis Res Ther 2011;13:R134.
24. Manolescu D, Davidescu L, Traila D, Oancea C, Tudorache V. The reliability of lung ultrasound in assessment of idiopathic pulmonary fibrosis. Clin Interv Aging 2018;13:437-49.
25. Gargani L, Doveri M, D'Errico L, Frassi F, Bazzichi ML, Delle Sedie A, Scali MC, Monti S, Mondillo S, Bombardieri S, Caramella D, Picano E. Ultrasound lung comets in systemic sclerosis: a chest sonography hallmark of pulmonary interstitial fibrosis. Rheumatology (Oxford) 2009;48:1382-7.
26. Vassalou EE, Raissaki M, Magkanas E, Antoniou KM, Karantanas AH. Lung Ultrasonography in Patients With Idiopathic Pulmonary Fibrosis: Evaluation of a Simplified Protocol With High-Resolution Computed Tomographic Correlation. J Ultrasound Med 2018;37:689-96.
27. Warrick JH, Bhalla M, Schabel SI, Silver RM. High resolution computed tomography in early scleroderma lung disease. J Rheumatol 1991;18:1520-8.
28. Ferraioli G, Tinelli C, Zicchetti M, Above E, Poma G, Di Gregorio M, Filice C. Reproducibility of real-time shear

wave elastography in the evaluation of liver elasticity. Eur J Radiol 2012;81:3102-6.
29. Hong S, Woo OH, Shin HS, Hwang SY, Cho KR, Seo BK. Reproducibility and diagnostic performance of shear wave elastography in evaluating breast solid mass. Clin Imaging 2017;44:42-5.
30. Xiang X, Yan F, Yang Y, Tang Y, Wang L, Zeng J, Qiu L. Quantitative Assessment of Healthy Skin Elasticity: Reliability and Feasibility of Shear Wave Elastography. Ultrasound Med Biol 2017;43:445-52.
31. Moazedi-Fuerst FC, Zechner PM, Tripolt NJ, Kielhauser SM, Brickmann K, Scheidl S, Lutfi A, Graninger WG. Pulmonary echography in systemic sclerosis. Clin Rheumatol 2012;31:1621-5.
32. Buda N, Piskunowicz M, Porzezińska M, Kosiak W, Zdrojewski Z. Lung Ultrasonography in the Evaluation of Interstitial Lung Disease in Systemic Connective Tissue Diseases: Criteria and Severity of Pulmonary Fibrosis - Analysis of 52 Patients. Ultraschall Med 2016;37:379-85.
33. Zhou B, Bartholmai BJ, Kalra S, Osborn TG, Zhang X. Lung US Surface Wave Elastography in Interstitial Lung Disease Staging. Radiology 2019;291:479-84.
34. Zhang X, Zhou B, Kalra S, Bartholmai B, Greenleaf J, Osborn T. An Ultrasound Surface Wave Technique for Assessing Skin and Lung Diseases. Ultrasound Med Biol 2018;44:321-31.

Cite this article as: Huang S, Guo R, Yuan X, Tang X, Liu T, Xie Q, Qiu L. Evaluation of connective tissue disease-related interstitial lung disease using ultrasound elastography: a preliminary study. Quant Imaging Med Surg 2022;12(7):3778-3791. doi: 10.21037/qims-21-1205

Supplementary

Table S1 Comparison of lung ultrasound measurements of the right lung between the case group and the control group

Right lung	The number of B-lines			H (mm)		
	Case group (n=65)	Control group (n=60)	P	Case group (n=65)	Control group (n=60)	P
Parasternal line						
2nd LIS	0.00 (0.00, 3.00)	0.00 (0.00, 0.00)	<0.001*	1.10 (0.80, 1.30)	0.70 (0.60, 0.70)	<0.001*
3rd LIS	0.00 (0.00, 2.00)	0.00 (0.00, 0.00)	<0.001*	0.90 (0.80, 1.10)	0.70 (0.60, 0.80)	<0.001*
4th LIS	0.00 (0.00, 2.00)	0.00 (0.00, 0.00)	<0.001*	0.80 (0.70, 1.00)	0.80 (0.70, 0.80)	<0.001*
5th LIS	0.00 (0.00, 2.75)	0.00 (0.00, 0.00)	<0.001*	0.95 (0.80, 1.18)	0.75 (0.70, 0.80)	<0.001*
Midclavicular line						
2nd LIS	0.00 (0.00, 4.00)	0.00 (0.00, 0.00)	<0.001*	1.10 (0.80, 1.40)	0.70 (0.60, 0.80)	<0.001*
3rd LIS	0.00 (0.00, 3.00)	0.00 (0.00, 0.00)	<0.001*	0.90 (0.80, 1.30)	0.70 (0.70, 0.80)	<0.001*
4th LIS	0.00 (0.00, 3.00)	0.00 (0.00, 0.00)	<0.001*	1.00 (0.80, 1.40)	0.70 (0.70, 0.80)	<0.001*
5th LIS	0.00 (0.00, 2.50)	0.00 (0.00, 0.00)	<0.001*	1.10 (0.90, 1.40)	0.70 (0.70, 0.80)	<0.001*
Anterior axillary line						
2nd LIS	0.00 (0.00, 5.00)	0.00 (0.00, 0.00)	<0.001*	1.20 (0.90, 1.40)	0.70 (0.70, 0.80)	<0.001*
3rd LIS	0.00 (0.00, 4.00)	0.00 (0.00, 0.00)	<0.001*	1.10 (0.80, 1.40)	0.70 (0.70, 0.80)	<0.001*
4th LIS	0.00 (0.00, 3.25)	0.00 (0.00, 0.00)	<0.001*	1.10 (0.80, 1.40)	0.70 (0.70, 0.80)	<0.001*
5th LIS	0.00 (0.00, 3.00)	0.00 (0.00, 0.00)	<0.001*	1.10 (0.90, 1.50)	0.80 (0.70, 0.80)	<0.001*
Midaxillary line						
2nd LIS	0.00 (0.00, 4.00)	0.00 (0.00, 0.00)	<0.001*	1.20 (1.00, 1.60)	0.80 (0.70, 0.90)	<0.001*
3rd LIS	0.00 (0.00, 1.00)	0.00 (0.00, 0.00)	<0.001*	1.10 (0.90, 1.30)	0.80 (0.70, 0.80)	<0.001*
4th LIS	0.00 (0.00, 2.00)	0.00 (0.00, 0.00)	<0.001*	1.10 (0.80, 1.40)	0.80 (0.70, 0.83)	<0.001*
5th LIS	0.00 (0.00, 3.00)	0.00 (0.00, 0.00)	<0.001*	1.10 (0.90, 1.45)	0.80 (0.70, 0.90)	<0.001*
Posterior axillary line						
7th LIS	0.00 (0.00, 3.00)	0.00 (0.00, 0.00)	<0.001*	1.30 (0.90, 1.50)	0.70 (0.70, 0.80)	<0.001*
8th LIS	0.00 (0.00, 3.00)	0.00 (0.00, 0.00)	<0.001*	1.30 (1.00, 1.65)	0.70 (0.70, 0.80)	<0.001*
Subscapular line						
7th LIS	0.00 (0.00, 3.00)	0.00 (0.00, 0.00)	<0.001*	1.20 (0.90, 1.60)	0.70 (0.70, 0.80)	<0.001*
8th LIS	0.00 (0.00, 4.75)	0.00 (0.00, 0.00)	<0.001*	1.30 (1.00, 1.60)	0.70 (0.70, 0.80)	<0.001*
Paravertebral line						
2nd LIS	0.00 (0.00, 0.00)	0.00 (0.00, 0.00)	<0.001*	1.00 (0.80, 1.20)	0.70 (0.70, 0.73)	<0.001*
3rd LIS	0.00 (0.00, 0.00)	0.00 (0.00, 0.00)	<0.001*	1.00 (0.80, 1.20)	0.70 (0.70, 0.80)	<0.001*
4th LIS	0.00 (0.00, 0.00)	0.00 (0.00, 0.00)	<0.001*	1.00 (0.80, 1.30)	0.70 (0.70, 0.80)	<0.001*
5th LIS	0.00 (0.00, 1.00)	0.00 (0.00, 0.00)	<0.001*	1.10 (0.80, 1.50)	0.70 (0.70, 0.80)	<0.001*
6th LIS	0.00 (0.00, 1.00)	0.00 (0.00, 0.00)	<0.001*	1.20 (1.00, 1.60)	0.70 (0.70, 0.80)	<0.001*
7th LIS	0.00 (0.00, 2.00)	0.00 (0.00, 0.00)	<0.001*	1.30 (1.00, 1.50)	0.80 (0.70, 0.80)	<0.001*
8th LIS	0.00 (0.00, 3.00)	0.00 (0.00, 0.00)	<0.001*	1.40 (1.10, 1.70)	0.80 (0.70, 0.80)	<0.001*

Data are presented as the median (upper quartile, lower quartile); H, pleural line thickness; LIS, lung intercostal spaces. *P<0.001.

https://dx.doi.org/10.21037/qims-21-1205

Table S2 Comparison of lung ultrasound measurements of the left lung between the case group and the control group

Left lung	The number of B-lines			H (mm)		
	Case group (n=65)	Control group (n=60)	P	Case group (n=65)	Control group (n=60)	P
Parasternal line						
2nd LIS	0.00 (0.00, 1.50)	0.00 (0.00, 0.00)	<0.001*	0.80 (0.70, 1.00)	0.60 (0.60, 0.70)	<0.001*
3rd LIS	0.00 (0.00, 1.00)	0.00 (0.00, 0.00)	<0.001*	0.80 (0.70, 1.00)	0.60 (0.60, 0.70)	<0.001*
4th LIS	0.00 (0.00, 0.00)	0.00 (0.00, 0.00)	<0.001*	0.85 (0.80, 1.00)	0.70 (0.60, 0.70)	<0.001*
Midclavicular line						
2nd LIS	0.00 (0.00, 3.00)	0.00 (0.00, 0.00)	<0.001*	0.90 (0.70, 1.20)	0.60 (0.60, 0.70)	<0.001*
3rd LIS	0.00 (0.00, 3.00)	0.00 (0.00, 0.00)	<0.001*	0.90 (0.70, 1.10)	0.70 (0.60, 0.70)	<0.001*
4th LIS	0.00 (0.00, 3.00)	0.00 (0.00, 0.00)	<0.001*	1.00 (0.80, 1.20)	0.70 (0.60, 0.70)	<0.001*
Anterior axillary line						
2nd LIS	0.00 (0.00, 3.00)	0.00 (0.00, 0.00)	<0.001*	1.10 (0.90, 1.30)	0.70 (0.70, 0.80)	<0.001*
3rd LIS	0.00 (0.00, 4.00)	0.00 (0.00, 0.00)	<0.001*	1.10 (0.80, 1.30)	0.70 (0.70, 0.80)	<0.001*
4th LIS	0.00 (0.00, 3.00)	0.00 (0.00, 0.00)	<0.001*	1.00 (0.85, 1.40)	0.70 (0.70, 0.80)	<0.001*
Midaxillary line						
2nd LIS	0.00 (0.00, 3.00)	0.00 (0.00, 0.00)	<0.001*	1.20 (0.90, 1.60)	0.80 (0.70, 0.90)	<0.001*
3rd LIS	0.00 (0.00, 2.00)	0.00 (0.00, 0.00)	<0.001*	1.10 (0.80, 1.30)	0.75 (0.70, 0.80)	<0.001*
4th LIS	0.00 (0.00, 3.00)	0.00 (0.00, 0.00)	<0.001*	1.05 (0.88, 1.40)	0.80 (0.70, 0.80)	<0.001*
Posterior axillary line						
7th LIS	0.00 (0.00, 2.25)	0.00 (0.00, 0.00)	<0.001*	1.30 (1.00, 1.80)	0.70 (0.70, 0.80)	<0.001*
8th LIS	0.00 (0.00, 3.00)	0.00 (0.00, 0.00)	<0.001*	1.40 (1.10, 1.90)	0.70 (0.70, 0.80)	<0.001*
Subscapular line						
7th LIS	0.00 (0.00, 4.00)	0.00 (0.00, 0.00)	<0.001*	1.30 (1.10, 1.70)	0.75 (0.70, 0.80)	<0.001*
8th LIS	0.00 (0.00, 5.00)	0.00 (0.00, 0.00)	<0.001*	1.40 (1.10, 1.80)	0.80 (0.70, 0.80)	<0.001*
Paravertebral line						
2nd LIS	0.00 (0.00, 0.00)	0.00 (0.00, 0.00)	<0.001*	0.95 (0.80, 1.20)	0.70 (0.70, 0.80)	<0.001*
3rd LIS	0.00 (0.00, 0.00)	0.00 (0.00, 0.00)	<0.001*	1.00 (0.80, 1.23)	0.70 (0.70, 0.80)	<0.001*
4th LIS	0.00 (0.00, 0.00)	0.00 (0.00, 0.00)	<0.001*	1.00 (0.80, 1.30)	0.70 (0.70, 0.80)	<0.001*
5th LIS	0.00 (0.00, 1.00)	0.00 (0.00, 0.00)	<0.001*	1.30 (0.90, 1.50)	0.80 (0.70, 0.80)	<0.001*
6th LIS	0.00 (0.00, 2.00)	0.00 (0.00, 0.00)	<0.001*	1.20 (1.00, 1.60)	0.80 (0.70, 0.80)	<0.001*
7th LIS	0.00 (0.00, 2.00)	0.00 (0.00, 0.00)	<0.001*	1.30 (1.00, 1.70)	0.80 (0.70, 0.80)	<0.001*
8th LIS	0.00 (0.00, 3.00)	0.00 (0.00, 0.00)	<0.001*	1.30 (1.10, 1.80)	0.80 (0.78, 0.90)	<0.001*

Data are presented as the median (upper quartile, lower quartile); H, pleural line thickness; LIS, lung intercostal spaces. *P<0.001.

https://dx.doi.org/10.21037/qims-21-1205

Table S3 Comparison of shear wave elastography measurements of the right lung between the case group and the control group

Right lung	Emean (kPa)			Cmean (m/s)		
	Case group (n=65)	Control group (n=60)	P	Case group (n=65)	Control group (n=60)	P
Parasternal line						
2nd LIS	11.17 (8.67, 18.30)	13.20 (8.08, 18.08)	0.876	1.90 (1.70, 2.43)	2.10 (1.60, 2.43)	0.736
3rd LIS	16.10 (9.87, 21.03)	12.40 (8.88, 18.10)	0.054	2.30 (1.80, 2.63)	2.00 (1.68, 2.43)	0.042
4th LIS	15.33 (10.85, 24.52)	14.15 (10.08, 18.60)	0.205	2.23 (1.88, 2.83)	2.15 (1.80, 2.50)	0.201
5th LIS	18.38 (14.67, 26.98)	14.25 (10.90, 18.68)	0.007*	2.45 (2.07, 3.00)	2.20 (1.90, 2.50)	0.008*
Midclavicular line						
2nd LIS	18.63 (14.67, 29.37)	16.30 (12.10, 20.70)	0.021*	2.47 (2.20, 3.10)	2.30 (2.00, 2.60)	0.021*
3rd LIS	20.57 (13.87, 26.77)	16.10 (13.75, 18.28)	0.017*	2.60 (2.13, 3.00)	2.30 (2.10, 2.50)	0.018*
4th LIS	20.90 (15.33, 26.07)	16.45 (14.38, 18.63)	0.001*	2.67 (2.27, 2.97)	2.30 (2.18, 2.50)	0.001*
5th LIS	20.93 (15.10, 28.67)	16.00 (14.30, 18.80)	<0.001*	2.67 (2.20, 3.10)	2.30 (2.20, 2.50)	0.001*
Anterior axillary line						
2nd LIS	17.07(13.03, 23.40)	15.90 (12.58, 17.05)	0.054	2.40 (2.07, 2.80)	2.30 (2.00, 2.40)	0.046*
3rd LIS	16.13(12.13, 21.80)	14.50 (11.98, 17.30)	0.236	2.33 (2.00, 2.67)	2.20 (2.00, 2.40)	0.214
4th LIS	16.22(12.42, 24.34)	15.30 (12.25, 18.63)	0.432	2.27 (2.03, 2.78)	2.20 (2.00, 2.50)	0.434
5th LIS	18.47(14.43, 25.19)	15.85 (13.80, 18.68)	0.026*	2.45 (2.20, 2.90)	2.30 (2.18, 2.50)	0.036*
Midaxillary line						
2nd LIS	16.53 (11.70, 19.57)	15.50 (13.08, 17.60)	0.949	2.30 (1.93, 2.53)	2.30 (2.10, 2.40)	0.943
3rd LIS	15.60 (10.77, 24.30)	14.70 (12.30,16.90)	0.460	2.23 (1.90, 2.87)	2.20 (2.00, 2.40)	0.582
4th LIS	16.83 (13.60, 24.00)	15.10 (12.65, 17.15)	0.022*	2.37 (2.13, 2.83)	2.20 (2.00, 2.40)	0.025*
5th LIS	17.67 (12.49, 23.56)	15.30 (13.68, 17.45)	0.059	2.40 (2.02, 2.83)	2.20 (2.10, 2.40)	0.062
Posterior axillary line						
7th LIS	16.80 (10.32, 21.41)	14.75 (11.73, 17.88)	0.295	2.32 (1.81, 2.63)	2.20 (1.98, 2.40)	0.364
8th LIS	17.83 (13.17, 22.80)	14.25 (12.08, 16.30)	0.002*	2.43 (2.07, 2.73)	2.20 (2.00, 2.30)	0.004*
Subscapular line						
7th LIS	17.00 (10.17, 21.73)	15.15 (12.18, 17.65)	0.212	2.30 (1.83, 2.67)	2.20 (2.00, 2.40)	0.213
8th LIS	15.78 (10.52, 22.49)	14.20 (11.98, 18.63)	0.631	2.27 (1.85, 2.69)	2.15 (2.00, 2.50)	0.535
Paravertebral line						
2nd LIS	27.90 (17.60, 39.72)	15.40 (12.45, 18.13)	<0.001*	3.00 (2.40, 3.53)	2.20 (2.00, 2.40)	<0.001*
3rd LIS	26.70 (13.88, 37.62)	15.55 (12.48, 18.68)	<0.001*	2.98 (2.13, 3.52)	2.30 (2.00, 2.50)	<0.001*
4th LIS	18.63 (12.43, 29.53)	16.95 (12.60, 18.85)	0.031*	2.47 (2.03, 3.13)	2.40 (2.00, 2.50)	0.035*
5th LIS	18.97 (10.70, 27.17)	14.40 (10.78, 17.40)	0.042*	2.50 (1.87, 3.00)	2.20 (1.90, 2.40)	0.052
6th LIS	14.93 (8.83, 22.70)	14.80 (12.33, 18.20)	0.763	2.20 (1.70, 2.67)	2.20 (2.00, 2.50)	0.876
7th LIS	15.90 (10.17, 20.93)	14.75 (12.08, 18.20)	0.925	2.17 (1.80, 2.63)	2.20 (2.00, 2.50)	0.898
8th LIS	13.67 (7.70, 19.90)	14.90 (13.00, 17.48)	0.226	2.10 (1.57, 2.57)	2.20 (2.00, 2.40)	0.290

Data are presented as the median (upper quartile, lower quartile). Emean, averaged mean Young's modulus; Cmean, averaged mean shear wave velocity; LIS, lung intercostal spaces; *P<0.001.

https://dx.doi.org/10.21037/qims-21-1205

Table S4 Comparison of shear wave elastography measurements of the left lung between the case group and the control group

Left lung	Emean (kPa)			Cmean (m/s)		
	Case group (n=65)	Control group (n=60)	P	Case group (n=65)	Control group (n=60)	P
Parasternal line						
2nd LIS	12.53 (8.72, 17.58)	11.90 (8.23, 16.83)	0.493	2.03 (1.70, 2.37)	2.00 (1.60, 2.30)	0.536
3rd LIS	19.78 (9.98, 33.75)	14.85 (12.95, 20.13)	0.070	2.57 (1.80, 3.36)	2.20 (2.08, 2.50)	0.069
4th LIS	21.20 (12.75, 28.06)	16.70 (13.75, 23.00)	0.121	2.62 (1.95, 3.03)	2.30 (2.10, 2.70)	0.133
Midclavicular line						
2nd LIS	23.10 (16.97, 34.40)	18.05 (14.63, 22.15)	0.001*	2.83 (2.37, 3.37)	2.45 (2.20, 2.70)	0.001*
3rd LIS	21.83 (16.82, 29.09)	17.05 (14.38, 20.45)	<0.001*	2.70 (2.39, 3.11)	2.40 (2.20, 2.63)	<0.001*
4th LIS	21.37 (15.60, 27.80)	16.55 (13.68, 18.90)	<0.001*	2.67 (2.27, 3.03)	2.30 (2.10, 2.50)	<0.001*
Anterior axillary line						
2nd LIS	17.40 (13.50, 21.97)	15.45 (12.35, 18.33)	0.053	2.43 (2.10, 2.70)	2.30 (2.00, 2.50)	0.032*
3rd LIS	18.93 (13.80, 22.20)	15.45 (13.00, 11.60)	0.020*	2.47 (2.17, 2.73)	2.25 (2.10, 2.40)	0.018*
4th LIS	18.23 (14.75, 23.58)	14.95 (11.60, 17.33)	<0.001*	2.47 (2.18, 2.78)	2.20 (1.98, 2.40)	<0.001*
Midaxillary line						
2nd LIS	17.07 (13.33, 23.80)	15.90 (12.78, 18.35)	0.052	2.37 (2.10, 2.83)	2.30 (2.00, 2.50)	0.048*
3rd LIS	18.67 (12.97, 25.20)	15.70 (13.10, 18.25)	0.072	2.50 (2.07, 2.90)	2.30 (2.10, 2.50)	0.072
4th LIS	18.85 (14.77, 25.21)	15.75 (13.35, 18.25)	0.003*	2.50 (2.17, 2.91)	2.30 (2.10, 2.50)	0.004*
Posterior axillary line						
7th LIS	14.85 (10.37, 22.87)	14.65 (11.50, 18.65)	0.447	2.20 (1.83, 2.73)	2.20 (1.90, 2.50)	0.514
8th LIS	16.93 (11.90, 23.10)	14.25 (11.98, 17.63)	0.107	2.33 (1.97, 2.73)	2.20 (2.00, 2.40)	0.190
Subscapular line						
7th LIS	16.53 (11.30, 24.33)	15.40 (11.70, 17.93)	0.239	2.33 (1.90, 2.83)	2.25 (1.98, 2.40)	0.306
8th LIS	11.97 (7.67, 20.90)	15.95 (12.28, 18.95)	0.341	1.97 (1.58, 2.63)	2.30 (2.00, 2.50)	0.305
Paravertebral line						
2nd LIS	28.23 (15.80, 38.42)	15.50 (10.65, 18.28)	<0.001*	3.05 (2.27, 3.58)	2.25 (1.88, 2.50)	<0.001*
3rd LIS	24.08 (19.03, 31.97)	15.05 (12.88, 18.33)	<0.001*	2.77 (2.46, 3.25)	2.20 (2.08, 2.43)	<0.001*
4th LIS	20.87 (16.93, 34.03)	15.70 (12.90, 18.53)	<0.001*	2.60 (2.27, 3.33)	2.25 (2.00, 2.50)	<0.001*
5th LIS	18.73 (14.47, 29.80)	15.25 (12.80, 18.63)	0.001*	2.50 (2.20, 3.13)	2.20 (2.00, 2.50)	0.001*
6th LIS	17.53 (12.73, 28.10)	15.55 (11.85, 18.38)	0.034*	2.40 (2.03, 3.00)	2.20 (1.98 2.50)	0.028*
7th LIS	14.97 (10.77, 24.00)	14.65 (11.20, 17.70)	0.349	2.17 (1.90, 2.80)	2.20 (1.90, 2.40)	0.365
8th LIS	15.13 (9.53, 22.50)	14.55 (12.28, 18.15)	0.693	2.23 (1.77, 2.70)	2.20 (2.00, 2.50)	0.966

Data are presented as the median (upper quartile, lower quartile). Emean, averaged mean Young's modulus; Cmean, averaged mean shear wave velocity; LIS, lung intercostal spaces. *P<0.001.

https://dx.doi.org/10.21037/qims-21-1205